Journal of Organometallic Chemistry, 474 (1994) 117–122

Novel concepts in directed biaryl synthesis

XXXIII *. An EXAFS spectroscopic study of the structure of lactone-bridged biaryls coordinated to $CpZrCl_3$ in toluene solution

F. Bökman [a,b], H, Bertagnolli [a], O. Schupp [c] and G. Bringmann [c]

[a] *Institute of Physical Chemistry II, University of Stuttgart, Postfach, D-70511 Stuttgart (Germany)*
[b] *Department of Organic Chemistry, Uppsala University, P.O. Box 531, S-751 21 Uppsala (Sweden)*
[c] *Department of Organic Chemistry, University of Würzburg, Am Hubland, D-97074 Würzburg (Germany)*

(Received July 29, 1993)

Abstract

The adduct formed between $CpZrCl_3$ and a biaryl lactone has been studied in toluene solution by Zr K X-ray absorption spectroscopy. The adduct is dimeric in toluene, as evidenced by a long Zr–Zr distance of 3.76 Å. In the dimer $[CpZrCl_2(\text{lactone } \mathbf{1d})(\mu\text{-Cl})]_2$, each zirconium centre is pseudo-octahedrally coordinated with the lactone carbonyl oxygen coordinated to the metal at a distance of 2.14 Å.

Key words: Zirconium; Cyclopentadienyl; Lactone; Bridging ligand; Biaryl; EXAFS

1. Introduction

Biaryl systems that are chiral as a result of steric hindrance are of great importance as pharmacologically active natural products and as useful reagents for asymmetric synthesis. The development of effective stereoselective synthetic routes to these compounds [2,3] is thus important for organic chemists.

We have developed a new approach to the synthesis of even highly *ortho*-substituted, and thus chiral biaryls, which in a very efficient way solves consecutively the two synthetic problems presented [4–6]. In this the aryl–aryl coupling is controlled by the use of artificial bridges, *e.g.* by ester functionalities, and asymmetric induction is achieved during the subsequent ring-opening of the lactone bridge, *e.g.* of compound **1**. This has been accomplished by atropisomer-selective ring-cleavage reactions of the lactone with chiral O- or N-nucleophiles [7] or with chiral hydride-transfer reagents [8–10].

Owing to the modest carbonyl reactivity of lactones of type **1**, most of the chiral nucleophiles previously employed had to be metal-activated, *i.e.* formally anionic. A significant improvement in this synthetic procedure might result if it could be extended to ring-opening reactions brought about by chiral non-charged nucleophiles, assisted by activation of the carbonyl group by Lewis acids. Furthermore, this might even lead to atropo-enantioselective ring-opening reactions involving use of cheap, achiral non-charged nucleophiles assisted by catalytic amounts of chiral Lewis acids. In initial experiments, the Lewis acid $CpZrCl_3$ [11], for example, was shown to form adducts with biaryl lactones [12].

The type of interaction between the Lewis acid and the lactone entity is naturally of great importance for the success of the planned asymmetric induction in these systems. Interesting questions are, for example, how strongly and at what distance the electron-deficient metal centre is bonded to the lactone, and to what extent there is a transfer of electronic charge to the metal ion. To gain an understanding of the nature of the complexation in these Lewis adducts of biaryl lactones, we have carried out X-ray absorption investigations of various systems of this type using the EXAFS method (extended X-ray absorption fine structure [13–15]). The species chosen were two adducts of lac-

---

Correspondence to: Dr. F. Bökman.

[*] For Part XXXII, see ref. 1.

[**] Dedicated to Professor Friedemann W. Schneider on the occasion of his 60th birthday.

0022-328X/94/$7.00
SSDI 0022-328X(93)24254-3

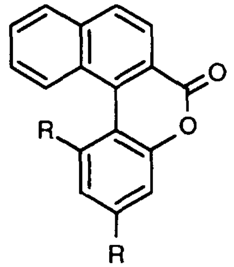

1

1	a	b	c	d
R	H	OMe	Me	O*n*Oct

tone biaryls with $CpZrCl_3$ in the solid state [12], a chiral rhenium lactone complex and the precursors of the latter in solution [16].

We describe below the EXAFS determination of the structure of an adduct between a zirconium-based Lewis acid and a biaryl lactone in solution, *viz.* that between $CpZrCl_3$ and lactone **1d**. To increase the solubility of the adduct in non-polar solvents, long aliphatic chains were introduced into the lactone. This gives rise to a sufficiently high solubility in the X-ray transparent solvent toluene to allow EXAFS measurements.

The characteristic property of EXAFS is that the local structure around only one atom type (in the present case zirconium) in the sample is probed, irrespective of whether the sample is a crystal, an amorphous solid or a liquid. This makes it especially suited for investigations of the local structures around metal ions in solution. Thus EXAFS studies, in combination with molecular mechanics studies and examination of the chemical reactivity, should help to find chemical species that meet the above-mentioned requirements in a more controlled and efficient way.

2. Experimental details

2.1. Preparation of the adduct $CpZrCl_3$/lactone 1d

A solution consisting of 325 mg (0.647 mmol) of lactone **1d** [17] in 10 ml of CH_2Cl_2 was added to a suspension of 170 mg (0.647 mmol) $CpZrCl_3$ [11] in 20 ml of CH_2Cl_2 at −78°C. The fluorescent green–yellow solution was allowed to warm to room temperature over a period of 5 h, the solvent was then removed and the residue dried under an oil pump vacuum to give a light yellow powder. IR (CH_2Cl_2) (cm^{-1}): 1620 (C=O); 1590, 1570, 1560 (C=C). ^1H NMR (200 MHz, CD_2Cl_2) δ: 0.80–1.85 (m, 30H, alkyl-H); 3.75 (m, 2H, O–CH_2–R); 4.00 (m, 2H, O–CH_2–R); 6.45 (s, br., 1H, 2-H or 4-H); 6.59 (s, br., 1H, 4-H or 2-H); 6.68 (s, 5H, C_5H_5); 7.57 (dd, 1H, $J = 7.4$ Hz, $J' = 6.9$ Hz, 10-H or 11-H); 7.77 (dd, 1H, $J = 7.6$ Hz, $J' = 6.9$ Hz, 11-H or 10-H); 7.90 (m, 2H, 9-H, 12-H); 8.17 (d, 1H, $J = 8.1$ Hz, 8-H); 8.47 (d, 1H, $J = 8.1$ Hz, 7-H) ppm. ^{13}C NMR (50 MHz, CD_2Cl_2) δ: 14.23, 14.29 (CH_3); 22.97, 23.09, 26.21, 26.33, 29.03, 29.10, 29.42, 29.48, 29.64, 29.73 (–CH_2–); 69.54, 70.03 (O–CH_2–); 93.95, 99.59 (2-C, 4-C); 103.56 (12c-C); 115.78 (12b-C); 120.81 (C_5H_5); 123.73 (6a-C); 125.63, 127.82, 128.03, 128.05, 129.70, 132.22 (7-C, 8-C, 9-C, 10-C, 11-C, 12-C); 131.49, 138.37 (8a-C, 12a-C); 152.98 (4a-C); 157.69, 163.17 (1-C, 3-C); 168.69 (C–O) ppm.

The solid was dissolved in 16 ml of toluene and the solution transferred to the sample cell under nitrogen gas. X-Ray absorption experiments were performed at station RÖMO II of HASYLAB (electron energy, 4.45 GeV; max. current, ~ 40 mA; beam half-life time, ~ 2 h; pre-edge, 5 eV steps; edge, 0.5 eV steps; post-edge, 0.06–0.08 $Å^{-1}$ steps; total scan times, ~ 30 min).

The Si(311) double-crystal monochromator with an entrance slit of ~ 1 mm height gave a spectrometer resolution of ~ 5 eV at 18 keV, comparable to the lifetime of the Zr K core hole (~ 5 eV [18]). Higher harmonics were rejected by means of a slight detuning of the monochromator (~ 40% intensity loss). A Zr metal foil was used for energy calibration in all runs (E(Zr K, metal) = 17998 eV [19]).

Data were collected in the transmission mode with argon-filled ion chambers. Measurements were performed at room temperature (~ 25°C) with the sample solution under N_2 atmosphere inside a stainless-steel cell with an *in situ* variable path length [20,21]. Teflon-coated Kapton foils (Du Pont, type 200 FN 011, a gift from Du Pont de Nemours (Deutschland) GmbH, Bad Homburg) were used as X-ray windows for the liquid sample cell.

The relatively low solubility of the sample in non-coordinating solvents required a compromise between edge jump and total absorption. For the solution employed, the chosen path length ($d = 20$ mm) gave an edge jump $J = d\Delta\mu$ of ~ 0.45 and a total absorption above the edge of ~ 80%.

3. Data analysis

The EXAFS data analysis used in this work follows standard procedures (see, for example, refs. 14, 15 and 22) and is only briefly described here *.

---

* The computer programs used in the data analysis were written by T.S. Ertel and U. Kolb, see refs. 20, 23 and 24.

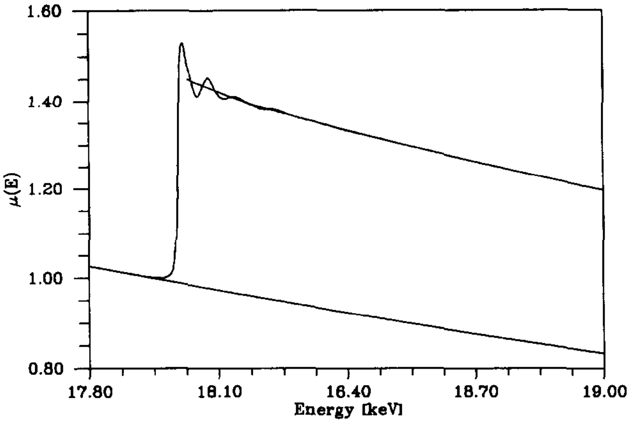

Fig. 1. Zr K X-ray absorption spectrum of a 1:1 mixture of $CpZrCl_3$ and lactone **1d** in toluene solution. Also shown are the pre- and post-edge backgrounds used in the data analysis.

The Zr K edges (E_0) of the transmission XAS spectra ($d\mu_{tot}(E) = \ln(I_0/I_{trans})$) were localized using the intersection method of Baldeschwieler *et al.* [25,26]. Two good spectra were averaged for the data analysis.

The pre-edge region was fitted with a Victoreen-type function [27] and the 'free atom'-like background was approximated with a smoothing spline [23,24,28–30] going from ~ 20 eV above the edge to the end of the spectrum (18950 eV). Figure 1 shows the total absorption together with the pre- and post-edge background functions while Fig. 2 shows the isolated EXAFS function $\chi(E)$.

The signal was converted from energy space to k-space, where the photo-electron wavenumber k is defined relative to the absorption energy E_0 by $k = [2m(E - E_0)/\hbar^2]^{1/2}$. The EXAFS, $\chi(k)$, was weighted by k^3 and Fourier-transformed to R-space, see Fig. 3 (dotted line). The Fourier transform was then back-transformed to k-space (with a square window R = 1.19–4.50 Å) in order to remove high-frequency noise and low-frequency oscillations remaining after the background subtraction (see Fig. 4, solid line).

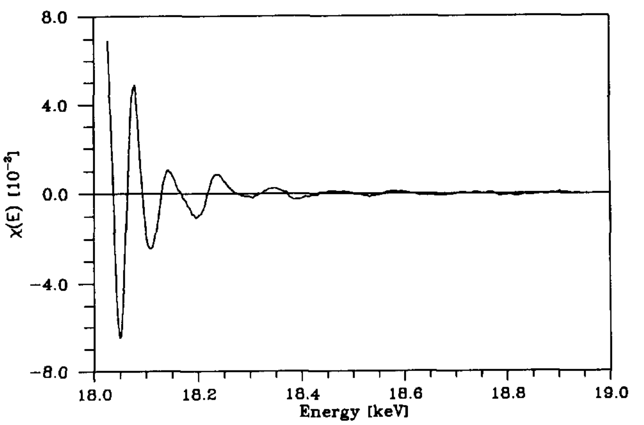

Fig. 2. Isolated EXAFS signal, $\chi(E)$.

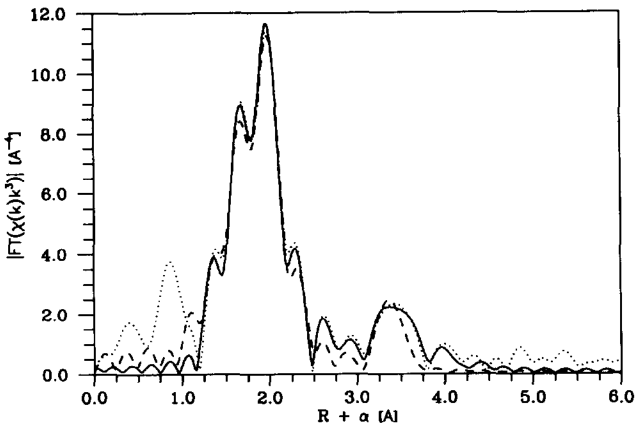

Fig. 3. Fourier transforms of the k^3-weighted experimental EXAFS spectrum (dotted line), the Fourier-filtered EXAFS spectrum (full line) and the best fit to the Fourier-filtered spectrum (dashed line).

The Fourier-filtered function $k^3\chi(k)$ was analyzed over the k-interval 2.35–15.66 Å^{-1} using a multiple shell curve-fitting program [20,24] with a theoretical EXAFS function of the form

$$\chi_{theory}(k) = S_0^2 A_0(k) \sum_{i=1}^{N_{shells}} N_i B_i(k) \frac{1}{kR_i^2} \exp\left(\frac{-2R_i}{\lambda(k)}\right) \times \exp(-2k^2\sigma_i^2) \times \sin(2kR_i + \phi_i(k) + \psi_0(k)). \tag{1}$$

Theoretical values for the parameters $B_i(k)$, $\phi_i(k)$, $\psi_0(k)$, $A_0(k)$ and $\lambda(k)$ (see, for example, refs. 22 and

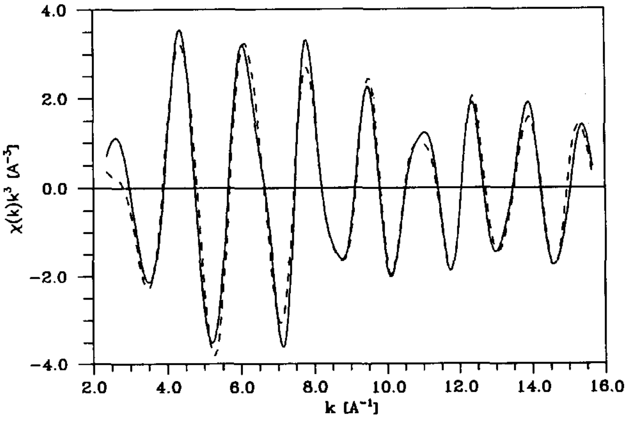

Fig. 4. Fourier-filtered and k^3-weighted experimental spectrum (full line) and best fit (dashed line).

31) were calculated for clusters of muffin-tin potentials with the program FEFF 4.06 of Rehr *et al.* [31,32] using a Hedin–Lundquist-type exchange potential.

In the multiple-shell curve-fitting, the distances $\{R_i\}$ of atoms of type i to the central zirconium atom and the Debye–Waller factors $\{\sigma_i\}$ of these distances were varied. The coordination numbers $\{N_i\}$ were kept constant for each structure considered. The parametric k-independent amplitude factor S_0^2 was also allowed to vary in the fits [31] and was normally 1.0 or slightly greater.

The number of free parameters that can be used in a multiple-shell curve-fitting procedure is limited by the number of independent points, $N_{\mathrm{idp}} \approx 2\Delta R\Delta k/\pi$. For this experiment Δk, the k-interval over which the fit is made, is ~ 13.3 Å^{-1}. The quantity ΔR, the R-interval over which the magnitude of the Fourier-transformed EXAFS is substantial, cannot be determined as unambiguously. If the window for the Fourier back-transformation is used, ΔR is ~ 3.3 Å and N_{idp} ~ 28. However, when the Fourier transform has one dominant peak followed by one or several smaller peaks, ΔR should cover more than the dominant peak, but less than the whole interval of interest. We estimate ΔR to be 1.5–2.0 Å, giving $N_{\mathrm{idp}} \approx$ 12–17. Thus, two limits for what can be fitted to the data are ($S_0^2 + 5 \times \{R_i, \sigma_i\} \rightarrow$ 11 parameters) and ($S_0^2 + 4 \times \{R_i, \sigma_i, E_{0,i}\} \rightarrow$ 13 parameters).

4. Results and discussion

The Zr K EXAFS spectrum of the $CpZrCl_3$/lactone **1d** adduct in toluene solution is shown in Fig. 1, the corresponding isolated EXAFS in Fig. 2 and the Fourier transform of the $k^3\chi(k)$ function in Fig. 3 (dotted line).

As can be seen from Fig. 3, there is a peak at a large radial distance, $R \approx 3.5$ Å (uncorrected for phase shifts), as also found in the EXAFS solid-state investigation reported earlier [12]. A peak at such a large distance from the central zirconium ion in a spectrum taken of a solution at room temperature is due either to (i) an atom with a high atomic number (higher back-scattering power and less thermal motion than low-Z atoms), (ii) an atom which is situated on a straight line from the central ion through some closer atom (the so-called 'focusing effect') or (iii) an atom in some rigid ligand (*e.g.* in a macrocycle). When the peak at $R \approx 3.5$ Å is filtered out from the rest of the signal (with a square window R = 3.06–3.82 Å), the resulting $k^3\chi(k)$ wave has an envelope characteristic of a heavy back-scatterer. Furthermore, the wave can be fitted very well with a single shell of one zirconium atom at a distance of 3.75 Å from the absorbing atom. Thus, it is clear that the peak is of type (i) and that the complex is dimeric in toluene solution, as found for the similar adduct in the solid state [12]. Accordingly, from the several structures tested, the best multiple-shell fit to the full Fourier-filtered spectrum (R = 1.19–4.50 Å) was obtained for the dimer $[CpZrCl_2(\text{lactone } \mathbf{1d})(\mu\text{-}Cl)]_2$.

TABLE 1. EXAFS results for $[CpZrCl_2(\text{lactone } \mathbf{1d})(\mu\text{-}Cl)]_2$ in toluene solution

	R (Å)	N [a]	σ (Å)	S_0^2	R_{solid} (Å) [b]
$[CpZrCl_2(\text{lactone})(\mu\text{-}Cl)]_2$				1.00	
O	2.14	1	0.053		2.11
Cl′	2.41	2	0.057		2.44
Cl″	2.57	2	0.106		2.71
C (Cp)	2.53	5	0.180		2.51
Zr	3.74	1	0.082		3.81

[a] Coordination numbers $\{N_i\}$ were kept fixed. [b] Another biaryl lactone, from ref. 12.

The best fit to the Fourier-filtered and k^3-weighted EXAFS spectrum is shown in Fig. 4, and Fig. 3 shows the Fourier transforms for these two $k^3\chi(k)$ functions (solid and broken lines). It can be seen that the fit reproduces the experimental data well, in both k- and R-space. The derived EXAFS parameters are listed in Table 1.

In this dimeric complex, each zirconium ion is pseudo-octahedrally coordinated, surrounded by two terminal chlorides (2.41 Å away), two bridging chlorides (2.62 Å), a cyclopentadienyl anion [R(Zr–C(Cp)) = 2.54 Å] and a lactone oxygen (2.14 Å). The other zirconium ion of the dimer is found at a distance of 3.76 Å from the central ion.

Thus, in the solution structure as determined by EXAFS, the zirconium–oxygen distance, 2.14 Å, lies between the X-ray crystallographic Zr^{4+}–O(carbonyl) distances of $[ZrCl_4(\text{n-hexyl acetate})]_2$ (2.112 Å) [33] and $ZrCl_4(\text{pinacolone})_2$ (2.191 Å) [34]. The solution Zr–O(biaryl lactone) distance is slightly longer than the corresponding distance in the EXAFS-determined solid-state structure [12] R(Zr–O) = 2.11 Å, possibly reflecting a decrease in steric strain in solution.

For a complex of the type $[CpZrCl_2(\text{lactone})(\mu\text{-}Cl)]_2$, there are 12 different isomers differing in whether both, one or none of the ligands Cp^- and lactone lie in the $Zr(\mu\text{-}Cl)_2$ plane and in the *cis–trans* relations of these ligands. Which configuration is the most stable around Zr^{4+} will depend both on electronic and local steric effects, and in the solid state on the crystal packing forces as well.

The Cp^- ligand is able to donate electronic charge efficiently into the Zr $4d_{xz}$ and $4d_{y'z}$ orbitals *. Thus,

---

* The vector Zr—Cp (centre) is taken as the local z-axis.

a ligand L that has poor donating properties in π-symmetry along the Zr—L bond would be more suitable in the position *trans* to Cp^- than a ligand that is a strong π-base. In the complex studied, a chloride ligand that σ-donates a lone pair to the Zr ion also has filled orbitals of π-symmetry available for donation, but a σ-donating carbonyl oxygen has not. * Hence, simple electronic arguments suggest that the dimer consists of an inorganic $Cl_2Zr(\mu\text{-}Cl)_2ZrCl_2$ plane with the organic ligands coordinated axially to the zirconium ions. The bulk of the biaryl lactone would then ensure that the two axial lactones are situated *trans* to each other. Such axial *trans* coordination of the carbonyl group is found, for example, in the crystal structures of dimeric $[TiCl_3(\text{ethyl acetate})(\mu\text{-}Cl)]_2$ [35] and $[ZrCl_3(\text{hexyl acetate})(\mu\text{-}Cl)]_2$ [33].

The different isomers would *in principle* have different numbers of groups of equivalent chlorides. For example, the isomer that we suggest on electronic grounds has two sets of chlorides, 2 × Cl(terminal) + 2 × Cl(bridging), in accordance with our EXAFS data analysis. We do not, however, take this as an argument for the suggested configuration. We did not try to split any of the two chloride shells since this would have resulted in too many free parameters. Furthermore, it would be difficult to make an unambiguous curve-fitting of many similar chloride shells even for an experiment with a better signal-to-noise ratio, *i.e.* with data extending further in *k*-space.

Finally, we note that the Zr K absorption edge of the $CpZrCl_3$ lactone **1d** adduct is shifted by *ca.* 5.3 eV to higher energy relative to the edge of the reference Zr metal foil. This shift is approximately 1 eV less than those for thf solutions of the complexes $CpZrCl_3(THF)_2$ and $ZrCl_4(THF)_2$ [36], probably owing to a greater charge donation to the Zr(IV) centre in the dimer.

Acknowledgments

We thank Dr C.L.J. Ewers for the preparation of lactone **1d**. Generous financial support of this work by the Deutsche Forschungsgemeinschaft (Sonderforschungsbereich No. 347 'Selective Reactions of Metal-Activated Molecules'), the Fonds der Chemischen Industrie and the Swedish Natural Science Research Council (F.B.) is gratefully acknowledged. The Hamburger Synchrotronstrahlungslabor (Hasylab am DESY) is thanked for providing access to synchrotron radiation.

References

1 K. Peters, E.-M. Peters, H.G. von Schnering, O. Schupp and G. Bringmann, *Z. Kristallogr.*, in press.
2 G. Bringmann, R. Walter and R. Weirich, *Angew. Chem., 102* (1990) 1006; *Angew. Chem., Int. Ed. Engl., 29* (1990) 977.
3 G. Bringmann, R. Walter and R. Weirich, in *Houben Weyl, Methods of Organic Chemistry*, E22, C2, in press.
4 G. Bringmann, L. Göbel and O. Schupp, *GIT Fachz. Lab.*, (1993) 189.
5 G. Bringmann, Ch. Ewers, L. Göbel, T. Hartung, L. Kinzinger, M. Schäffer, B. Schöner and O. Schupp, in H. Werner, A.G. Griesbeck, W. Adam, G. Bringmann and W. Kiefer (eds.), *Selective Reactions of Metal-Activated Molecules,* Vieweg, Braunschweig, 1992, p. 175.
6 G. Bringmann, Ch. Ewers, L. Göbel, T. Hartung, B. Schöner, O. Schupp and R. Walter, ref. 5, p. 183.
7 G. Bringmann, R. Walter and Ch. Ewers, *Synlett,* (1991) 581.
8 G. Bringmann and T. Hartung, *Synthesis,* (1992) 433.
9 G. Bringmann and T. Hartung, *Angew. Chem., 104* (1992) 782; *Angew. Chem., Int. Ed. Engl., 31* (1992) 761.
10 G. Bringmann and T. Hartung, *Tetrahedron, 49* (1993) 7891.
11 G. Erker, C. Sarter, M. Albrecht, S. Dehnicke, C. Krüger, E. Raabe, R. Schlund, R. Benn, A. Rufinska and R. Mynott, *J. Organomet. Chem., 382* (1990) 89.
12 T. Ertel, S. Hückmann, H. Bertagnolli, G. Bringmann, C. Ewers, G. Erker, I. Hart and C. Sarter, in S.S. Hasnain (ed.), *X-Ray Absorption Fine Structure,* Ellis Horwood Ltd., Chichester, 1991, p. 563.
13 D.C. Koningsberger and R. Prins (eds.), *X-Ray Absorption: Principles, Applications, Techniques of EXAFS, SEXAFS and XANES,* John Wiley & Sons, New York, 1988.
14 P.A. Lee, P.H. Citrin, P. Eisenberger and B.M. Kincaid, *Rev. Mod. Phys., 53* (1981) 769.
15 B.K. Teo, *EXAFS: Basic Principles and Data Analysis,* Springer-Verlag, Berlin, 1986.
16 R. Crüsemann, V. Fritsche, S. Hückmann, H. Bertagnolli, *Jpn. J. Appl. Phys., 32* (1993) 41, suppl. 32-2.
17 G. Bringmann, T. Hartung, L. Göbel, O. Schupp, C.L.J. Ewers, B. Schöner, R. Zagst, K. Peters, H.G. von Schnering and C. Burschka, *Liebigs Ann. Chem.,* (1992) 225.
18 O. Keski-Rahkonen and M.O. Krause, *At. Data Nucl. Data Tables, 14* (1974) 139.
19 G.P. Williams, in D. Vaughan (ed.), *X-ray Data Booklet,* Lawrence Berkeley Laboratory, Berkeley, 1986.
20 T.S. Ertel, *Ph.D. thesis,* Universität Würzburg, 1991.
21 T.S. Ertel and H. Bertagnolli, *Nucl. Instrum. Methods Phys. Res., Sect. B., B73* (1993) 199.
22 D.E. Sayers and B.A. Bunker, in D.C. Koningsberger and R. Prins (eds.), *X-Ray Absorption: Principles, Applications, Techniques of EXAFS, SEXAFS and XANES,* John Wiley&Sons, New York, 1988, Chap. 6.
23 U. Kolb, *Master's thesis,* Universität Würzburg, 1991.
24 T.S. Ertel, H. Bertagnolli, S. Hückmann, U. Kolb and D. Peter, *Appl. Spectrosc., 46* (1992) 690.

---

* This assumes an sp^2-hybridized carbonyl oxygen with two classically localized lone pairs and a C=O—Zr angle of ~120°. If the C=O—Zr angle is ~180°, the carbonyl group has one donating orbital of σ-type and one of π-type. On the other hand, when a carbonyl double bond σ-donates into empty zirconium orbitals there is a stabilization of the Cp—Zr $4d_{xz,yz}$ interaction due to the acceptor properties of the C=O π^*-orbital. Although the lactone must be η^1-coordinated to the extremely electron-poor Zr^{4+} ion, we have also tested η^2-coordination but these fits to the EXAFS data led to unrealistic results.

25 J.D. Baldeschwieler, F.G. Halaka and J.J. Boland, *Phys. Rev. B.,* *28* (1983) 2921.

26 F.G. Halaka, J.J. Boland and J.D. Baldeschwieler, *J. Am. Chem. Soc., 106* (1984) 5408.

27 J.A. Victoreen, *Appl. Phys., 18* (1948) 855.

28 C. Reinsch, *Num. Math., 10* (1967) 177.

29 *Fortran Subroutines for Mathematical Applications,* Version 1, IMSL Inc., Houston, 1987, subroutine ICSSV.

30 A. Proctor, M.J. Fay, D.P. Hoffmann and D.M. Hercules, *Appl. Spectrosc., 44* (1990) 1052.

31 J.J. Rehr, J. Mustre de Leon, S.I. Zabinsky and R.C. Albers, *J. Am. Chem. Soc., 113* (1991) 5135.

32 J. Mustre de Leon, J.J. Rehr, S.I. Zabinsky and R.C. Albers, *Phys. Rev. B., 44* (1991) 4146.

33 D.A. Young, *J. Mol. Catal., 88* (1988) 1405.

34 B. Galeffi, M. Simard and J.D. Wuest, *Inorg. Chem., 29* (1990) 951.

35 L. Brun, *Acta Crystallogr., 20* (1966) 739.

36 F. Bökman and H. Bertagnolli, *Hasylab Annual Report 1992,* Jan. 1993, p. 249.